European Review for Medical and Pharmacological Sciences 2024; 28: 3892-3904

Brain targeting efficacy of novel drug delivery system in the treatment of Alzheimer's disease

L.-H. DUAN[1,2], L.-M. LI[1,2], C.-B. WANG[3,4,5,6], Q.-Q. LIU[1,2], X. ZHANG[7], Z.-Z. WU[1,2,8]

[1]Department of Neurology, the First Affiliated Hospital of Shenzhen University, Shenzhen, China
[2]Shenzhen Institute of Geriatrics, Shenzhen, China
[3]Guangxi University of Science and Technology, Liuzhou, China
[4]South China University of Technology, Guangzhou, China
[5]Guangdong University of Science and Technology, Dongguan, China
[6]Guangdong MK Smart Robotics Co., Ltd, Zhuhai, China
[7]Neurorehabilitation Center, Shenzhen Dapeng New District Nan'Ao People's Hospital, Shenzhen, China
[8]Academician Wu Zhengzhi Workstation, Ningbo College of Health Sciences, Ningbo, China

ABSTRACT. – OBJECTIVE: Alzheimer's disease (AD), a common degenerative disease of the central nervous system in the elderly, has become the third largest health killer after cardiovascular and cerebrovascular diseases and tumors. Based on the fact that Alzheimer's disease is a disease with multiple etiologies and complex pathology, a single target is bound to have a limited curative effect, and the synergy of multiple links and multiple targets is expected to achieve a better curative effect. The aim of this study is to investigate the brain targeting of a drug modified by chitosan, based on the new nanodrug delivery system for treating Alzheimer's disease developed by the research group.

MATERIALS AND METHODS: Chitosan with good biocompatibility, biosorption, and degradation products that can protect and promote the regeneration of nerve cells was selected to combine with galantamine, a natural representative cholinesterase inhibitor, to develop a new nano drug delivery system for nasal delivery of anti-Alzheimer's disease with a multi-target synergistic effect. Synchronous analysis was conducted on the blood and brain tissue drug concentrations after intravenous and nasal administration of the original drug solution and system solution. The brain targeting index (DTI) is used to evaluate the brain targeting effect of the nano-drug delivery system after intranasal administration.

RESULTS: The blood concentration of galantamine original drug solution and galantamine system solution after intravenous injection and nasal show that in the two administration methods of intravenous injection and nasal administration, under the same administration method, the time point of the system reaching the highest blood drug concentration is much higher than that of the original drug. The content of galantamine in plasma samples and tissue samples indicate that after intravenous administration and intranasal administration of the galantamine system, at the same time point, the drug concentration in brain tissue was far greater than that of the original drug of galantamine, and the duration was also longer. The concentration of drugs in brain tissue decreased gradually in the order of olfactory bulb, olfactory tract, brain, and cerebellum. In the brain tissues of the olfactory bulb, olfactory tract, cerebrum, and cerebellum, the drug concentration of the galantamine system after intravenous injection is lower than that after nasal administration.

CONCLUSIONS: This study concludes that compared with the original drug solution, the nano drug delivery system has significant brain targeting for nasal administration, and intravenous injection also has brain targeting. In the olfactory bulb, olfactory tract, brain, and cerebellum, the brain targeting index at the olfactory bulb is the highest, and the targeting is the best.

Key Words:
Alzheimer's disease, Chitosan, Galantamine, Brain targeting, Neuropharmacological mechanism.

Introduction

Alzheimer's disease (AD), the first clinical case reported by German doctor Alois Alzheimer in 1906, is a neurodegenerative disease[1]. The proportion of Alzheimer's patients in dementia patients is 60-70%[2]. At this period, there are 50 million people with dementia, which is expected to reach 152 million in 2050[3]. Because Alzheimer's disease is spreading in both depth and breadth and has great

Corresponding Authors: Chunbao Wang, MD; e-mail: chunbaowang@163.com; Zhengzhi Wu, MD; e-mail: szwzz001@email.szu.edu.cn

harm to a certain extent, the patients encounter many obstacles in emotional personality, cognitive function, memory function, language function, visual space function, personal life self-care ability, social life ability, and so on[4-12]. Because of the substantial social burden caused by Alzheimer's disease[13], it has quickly emerged as a significant public health issue deserving widespread attention, with a certain impact on the overall social economy. At present, the drugs used for the clinical treatment of AD mainly include acetylcholinesterase (AchE) inhibitors[14], cerebral circulation improvers, neurotrophic factors[15], etc. Among them, acetylcholinesterase inhibitor drugs can be divided into four categories: (1) acetylcholine precursor acting on presynaptic, (2) acetylcholinesterase inhibitor acting on the synaptic space, (3) M1 receptor agonist which acts as a postsynaptic, (4) drugs that promote the release of acetylcholine[16]. Cholinesterase inhibitors reduce the degradation of acetylcholine by cholinesterase by inhibiting the activity of cholinesterase in the brain, thus increasing the content of acetylcholine in the brain, which is conducive to improving the learning and memory abilities of dementia patients[17]. Among the five anti-dementia drugs approved by the U.S. Food and Drug Administration, four are acetylcholinesterase inhibitors, including tacrine, donepezil, rivastigmine, and galanthamine[18]. Galanthamine was carried by the novel drug delivery system prepared in this paper.

The nasal drug delivery system is one of the drug delivery systems that have been studied extensively in recent years[19,20]. Drugs can reach the cerebrospinal fluid (CSF) or brain through the olfactory mucosa along the connecting tissues surrounding the olfactory nerve bundle or axons of olfactory neurons, so they can bypass the blood-brain barrier and enter the central nervous system and be directly absorbed into the brain. Drug delivery through the nasal cavity has the following characteristics[21-23]: quick onset, no injection is required, avoiding the first pass effect of the liver, and convenience to use the quantitative device.

Chitosan has biosorption, and its structure contains basic free amino and hydroxyl groups, which can form hydrogen bonds with glycoproteins in nasal mucus to produce adhesion, resist the clearance of drugs by mucosal cilia, and ensure the transmission of drugs across cell membranes[24,25]. In addition, the polymer chain is highly flexible, so it can effectively penetrate into the mucosal layer[2]. In the solution, chitosan can combine with hydrogen ions to create a positively charged molecular surface. This makes it easier to create a charged effect with the mucosal layer, allowing chitosan to absorb water and form a hydrogel, resulting in strong adhesion[24,25]. At the same time, chitosan can reversibly and temporarily open the tight connection between epithelial cells, enhance membrane permeability, and thus enhance the absorption of drugs by mucosa[26]. Furthermore, chitosan also has an anti-inflammatory effect[27-29], which can improve inflammation or damage of mucous membranes and avoid the impact of these conditions on drug absorption.

Therefore, in this paper, chitosan with good biocompatibility, biosorption, and degradation products that can protect and promote the regeneration of nerve cells was selected to combine with galantamine, a natural representative cholinesterase inhibitor, to develop a new nano drug delivery system for nasal delivery of anti-Alzheimer's disease with a multi-target synergistic effect. The effects of the composition of the drug delivery system on the loading efficiency and sustained-release rate of galantamine were investigated, with emphasis on nasal mucosal toxicity, nasal mucosal absorption, and brain targeting after chitosan modification.

Materials and Methods

Raw Materials

Galanthamine Hydrobromide (China National Institute for Food and Drug Control, Beijing, China). Chitosan (Molecular weight 1.2×10^5 g/mol, degree of deacetylation 88%, Shanghai Boao Biotechnology Co., Ltd, Shanghai, China). Polyethyleneimine, hydrogen peroxide, potassium periodate, sodium hydroxide, ethanol absolute, acetone, ethylene glycol, glacial acetic acid, sodium acetate, sodium borohydride, ammonia chloride, sodium chloride, triethylamine, phosphoric acid were of analytical grade (Guangzhou Chemical Reagent Factory, Guangzhou, Guangdong province, China).

Preparation of Nano-Drug Loading System

Aldehydes chitosan (CS-CHO) was oxidized to carboxylated chitosan (CS-COOH) with dimethyl sulfoxide (DMSO) as solvent and chlorite as oxidant. The products were dialyzed in NaCl aqueous solution and deionized water to remove impurities after being concentrated by rotary evaporation. The final product was freeze-dried. The structure of the product was identified by infrared spectrum analysis.

3893

Using DMSO as a solvent, CS-COOH was esterified with galantamine under the catalysis of N-(3-Dimethylaminopropyl)-N'-ethylcarbodiimide hydrochloride (EDC) and N-hydroxysuccinimide (NHS). After being concentrated by rotary evaporation, the product was dialyzed in NaCl aqueous solution and deionized water to remove impurities. The final product was freeze-dried. The structure of the product was identified by Fourier Transform infrared spectroscopy (FT-IR).

Animal Experiment

We employed simple randomization to assign 180 rats to each of the following groups. The rats were brought from Beijing Xinyuan Shunkang Technology Co. Ltd (Beijing, China).

Group I: Galantamine original drug solution-injected (37 rats).

Group II: Galantamine original drug solution-intranasal (41 rats).

Group III: Galantamine system solution-injected (49 rats).

Group IV: Galantamine system solution-intranasal (53 rats).

All rats were fasted for 24 hours prior to the experiment, although they had access to water. Within 30 minutes of receiving an intraperitoneal injection of 2% pentobarbital sodium solution (40 mg/kg) for anesthesia, the experiment commenced. Group I rats received the original drug solution and were euthanized at various time points: 5, 15, 30, 60, 90, 120, 240, 360, and 480 minutes post-administration (4 rats were sacrificed at each time point). Their samples were collected in heparinized anticoagulation centrifuge tubes. Similarly, Group II rats underwent intranasal administration of the drug and were euthanized at 2, 5, 15, 30, 60, 90, 120, 240, 360, and 480 minutes, and their samples were also collected in heparinized tubes. Additional collections for Group II occurred at 6, 8, 12, 24, and 36 hours post-administration. Group III and Group IV rats were euthanized at intervals similar to the previous groups following intravenous administration of the drug solution, with samples collected at the same specified time points.

Whole blood, centrifuged at 3,000 rpm for 15 min to separate plasma, cut skull, separate appropriate amount of olfactory bulb, olfactory tract, brain, and cerebellum, remove blood stains, accurately weigh, and add 0.1 mol/L Tris (Hydroxymethyl) Aminomethane Hydrochloride solution pH with a value of 10.0 at a ratio of 1:2 (W/V). Ultrasonically homogenized with a probe-type ultrasonic cell disruptor, and the plasma and brain tissue homogenized samples were frozen at -20°C for testing. Three rats were sacrificed at each time point.

Sample Determination

Plasma and brain tissue homogenate samples were frozen at -20°C and thawed at room temperature, and the content of galantamine was determined using the mature high-performance liquid chromatography method.

Data Processing and Pharmacokinetic Analysis

The nasal mucosal toxicity, nasal mucosal absorption were studied and the results were published on Shenzhen Journal of Integrated Traditional Chinese and Western Medicine in March 2020[30].

The blood drug concentration, brain tissue drug concentration and time data of different parts of each time point were listed, and the mean and standard deviation were calculated.

The main kinetic parameters were calculated using the 3P87 pharmacokinetic calculation program compiled by the Professional Committee of Mathematical Pharmacology of the Chinese Pharmacological Society. Among them, the concentration Cmax when the drug reaches the peak in the body and the time Tmax when it reaches the highest concentration were calculated from the measured values, and the area under the curve (AUC) was calculated by the linear trapezoidal area method.

The brain targeting index (DTI)[31,32] is used to evaluate the brain targeting effect of the nano-drug delivery system after intranasal administration. DTI is defined as the ratio of the area under the curve (AUC) of the drug in brain tissue to the AUC of the drug in plasma after intranasal administration and the ratio of the AUC of the drug in the brain tissue to the AUC of the drug in the plasma after intravenous administration, namely:

$$DTI = \frac{\left(AUC_{\text{brain tissue}} / AUC_{plasma}\right)_{\text{int}ranasal}}{\left(AUC_{\text{brain tissue}} / AUC_{plasma}\right)_{\text{int}ravenous}}$$

A DTI value greater than 1 indicates brain targeting, and the greater the DTI value, the stronger the brain targeting effect.

Statistical Analysis

GraphPad Prism software (version 8.0, San Diego, CA, USA) was used to perform the analysis.

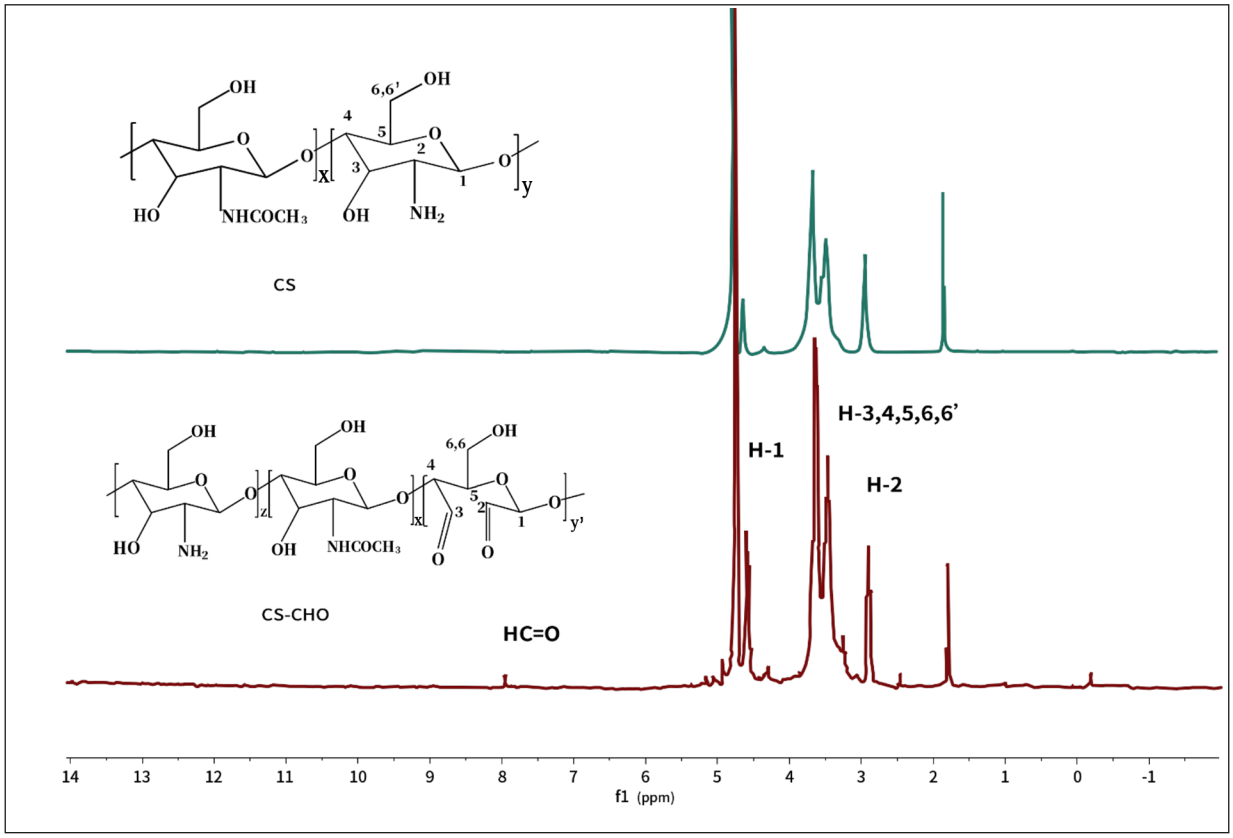

Figure 1. [1]H nuclear magnetic resonance (NMR) spectra of chitosan (CS) and aldehyde chitosan (CS-CHO).

The mean-standard deviation ($\bar{x}\pm s$) was used to represent the measurement data. Shapiro-Wilk normality test was used to confirm the validity and distribution of the data, using a One-way analysis of variance (ANOVA). One-way ANOVA followed by Tukey's post-hoc test was applied to groups for data analysis. Statistical significance was considered at $p<0.05$.

Results

Preparation of Nano-Drug Loading System of Aldehyde Chitosan (CS-CHO)

Periodate can oxidize the structure of cis o-diol to generate o-dialdehyde, which is often used to analyze the structure of carbohydrates. In addition, periodate can also be used to oxidize compounds with 1,2-dioxo group and 1,2-amino alcohol structure. The free amino group in the molecular structure of chitosan can be oxidized by periodate, while the acetylated amino group cannot participate in the reaction.

The solubility of the product was greatly increased after the aldehyde of chitosan and it could be completely dissolved in distilled water. This may be because the hydrogen bonds within and between CS molecules are destroyed after oxidation. The sugar ring is opened, thus improving the flexibility of the molecular chain, leading to improved solubility[33]. In addition, the decrease in CS molecular weight is also an important reason for the increase in solubility. The oxidation of CS by periodate will be accompanied by the degradation of CS, and the molecular weight of the obtained product will decrease, which may be related to the excessive oxidation of periodate (IO_4) and the attack of generated hydroxyl (OH) free radicals to the 1,4-glycosidic linkage in CS[34].

The water solubility and organic solvent solubility of CS-CHO are both increased, so the homogeneous reaction can be carried out in a neutral environment. In addition to the original hydroxyl and amino groups that can be further modified, a large number of aldehyde groups also can be further reacted.

The oxidation product CS-CHO was analyzed using Fourier transform infrared spectroscopy

Table I. Characterization of aldehyde chitosan (CS-CHO).

Sample	CS:KIO$_4$[a]	Yield/%	X[b]	R_{ua}/%[c]	Raldehyde/%
1	10:1	65	0.130	78.5	37.9
2	10:2	57	0.109	64.2	63.0
3	10:3	39	0.128	77.3	39.

[a]: $CS:KIO_4$ represents the molar ratio of chitosan and potassium periodate;

[b]: $X = \frac{I'_{H-2}}{I_{H-3,4,5,6,6'} - (I_{H-2} - I'_{H-2})}$, calculated from ^{1}H NMR; [c]: $R_{ua} = \frac{\frac{X}{0.160} - X}{1 - X}$.

(FI-IR) and nuclear magnetic resonance (NMR), respectively. It can be seen from the nuclear magnetic spectrum in Figure 1 that the chemical shift of H-3,4,5,6,6' in CS occurs at 3.3-3.8 ppm, H-1 at 4.6 ppm, and H-2 at about 2.8 ppm. In the spectrum of CS-CHO, the proton peak of the aldehyde group appears at 8.0 ppm, and the ratio of the integral area of H-3,4,5,6,6' to the integral area of H-2 increases from 4.58 of CS to 5.11. The reason is that the integral area of H-2 and H-3 (-3.0 ppm) decreases to the same extent after the oxidation of iodic acid. In contrast, the integral area of H-3,4,5,6,6' decreases to a lower extent than that of H-2, so the ratio increases.

From the infrared spectrum (Figure 2), it can be seen that chitosan has a bending vibration peak of amino at the wave number of 1,590 cm^{-1}, indicating that chitosan has free amino groups that have not been acylated, and 3,426 cm^{-1} is the absorption peak of hydroxyl. After CS was oxidized by potassium periodate, the characteristic peaks of 1,523 cm^{-1} and 1,640 cm^{-1} appeared, which were amide II peak and amide I peak, respectively. Moreover, there are two peaks with equal intensity at 2,760 and 2,780 cm^{-1}, and there is an absorption peak at 1,660 cm^{-1}, so it can be concluded that there is an aldehyde group on CS-CHO.

With different molar ratios of CS sugar ring and periodate, the following CS-CHO with different aldehyde degrees can be obtained using the same method, as shown in Table I.

Therefore, the molar ratio of chitosan and potassium periodate is 10:2, which has the highest degree of aldehyde.

Synthesis of Carboxylated Chitosan (CS-COOH)

It can be seen from Figure 3 that the stretching vibration peak of -OH and N-H at 3,424 cm^{-1}

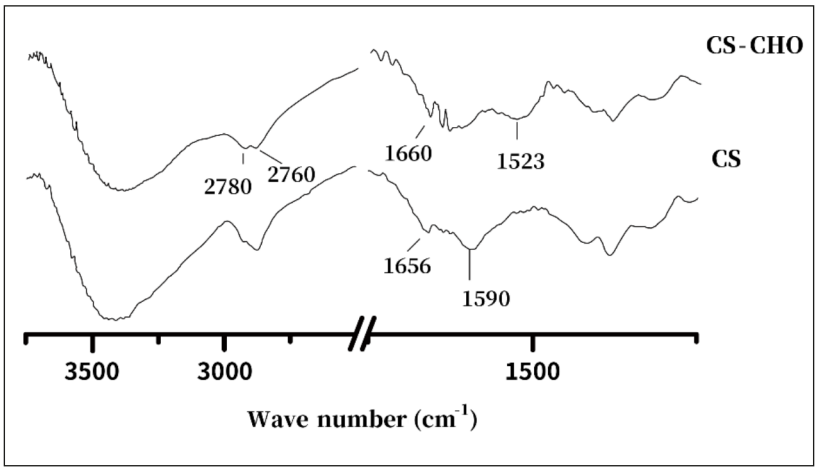

Figure 2. Fourier transform infrared spectroscopy (FI-IR) spectra of chitosan (CS) and aldehyde chitosan (CS-CHO).

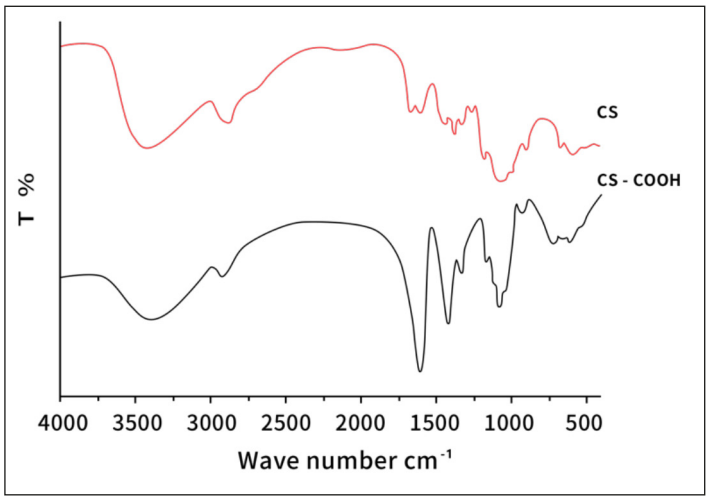

Figure 3. Infrared spectrogram of chitosan (CS) and carboxylated chitosan (CS-COOH).

in chitosan becomes wide and weak after modification, indicating that H on -OH and -NH_2 is replaced. The absorption peaks of the amide I band and amide II bands at 1,658 cm^{-1} and 1,597 cm^{-1} are fused into a single peak of 1,599 cm^{-1} after the substitution, indicating that the carboxyl group substituted the amide group. In addition, the strong absorption peak at 1,599 cm^{-1} and the middle absorption peak at 1,411 cm^{-1} are antisymmetric and symmetric stretching vibration peaks of carboxyl (COO), respectively.

Esterification of Carboxylated Chitosan with Galanthamine

Table II shows the change in the absorption peak of the infrared spectrum of carboxylated chitosan before and after esterification. The strong absorption peak at 1,599 cm^{-1} and the antisymmetric and symmetric stretching vibration peak of COO at 1,411 cm^{-1} become wide and weak after modification. After esterification, the absorption peak of keto carbonyl appears at 1,735 cm^{-1}.

Dynamic Changes of Plasma Concentration of Galantamine Nanosystem After Intravenous and Intranasal Administration

Galantamine original drug solution and system solution were administered intravenously and nasally to rats at a dose of 0.5 mg/kg, respectively. The plasma concentrations at different times are shown in Table III and Table IV.

It can be seen that after intravenous injection of galantamine original drug solution in rats, the plasma concentration of galantamine reaches the highest value at 2 minutes, and the blood concentration reaches the highest value at 30 minutes after intranasal administration. After intravenous injection of galantamine in rats, the plasma concentration of galantamine decreases rapidly within 30 minutes, and then the rate of decrease slows down.

After intravenous injection of galantamine system solution in rats, the plasma concentration gradually increases, reaching its highest value at

Table II. Peak changes of infrared spectrum before and after esterification of carboxylated chitosan.

Peak value cm^{-1}	Before esterification	After esterification
1,411	Present	Become wide and weak
1,599	Present	Become wide and weak
1,735	None	Present

Table III. Blood concentration of galantamine original drug solution after intravenous injection and nasal administration.

Time (min)	Intravenous injection (ng/mL)	Nasal administration (ng/mL)
2	5,546.86±647.24	–
5	2,517.34±994.32	104.65±19.12
15	1,481.36±420.47	167.65±14.23
30	870.68±301.75	653.90±153.06
60	731.94±144.20	455.60±157.06
90	599.43±27.22	355.50±30.84
120	319.40±10.18	308.45±102.59
240	95.38±18.79	259.55±49.16
360	37.65±11.07	189.65±41.65
480	–	55.20±4.00

Table IV. Blood concentration of galantamine system solution after intravenous injection and nasal administration.

Time	Intravenous injection (ng/mL)	Nasal administration (ng/mL)
2 min	11.34±4.52	–
5 min	28.53±8.62	11.35±4.41
15 min	92.53±13.52	29.00±6.25
30 min	171.52±36.52	25.27±3.51
60 min	210.26±38.41	80.83±26.35
90 min	248.95±42.34	150.05±32.16
120 min	422.35±43.43	173.31±43.13
240 min	715.56±46.15	210.10±54.55
6 h	1,575.53±68.35	634.89±64.29
8 h	3,458.34±351.57	1,323.35±136.32
12 h	5,038.14±115.14	2,937.90±271.23
24 h	2,525.25±134.24	4,331.39±151.01
36 h	1,291.55±162.56	2,123.92±99.34

12 h and its highest value at 24 h after intranasal administration.

Comparing Table III and Table IV, it can be seen that in the two administration methods of intravenous injection and nasal administration, under the same administration method, the time point of the system reaching the highest blood drug concentration is much higher than that of the original drug.

Galantamine original drug solution and galantamine system solution were administered intravenously and nasally to rats at a dose of 0.5 mg/kg, respectively. The drug concentration in brain tissue at different time and at different parts are shown in Table V to XII. Each trial was done three times.

The data above indicates that after intravenous administration, the original drug galantamine can only reach the brain at the first or second-time point. The drug concentration in different parts of the brain tissue (olfactory bulb, olfactory tract, brain, cerebellum) is similar. Subsequently, the concentration of the drug in the brain rapidly decreases along with the plasma concentration, and eventually falls below the detection limit.

After intranasal administration, although the blood drug concentration is much lower than that of intravenous injection, the drug concentration in brain tissue is much higher than that of intravenous injection, and the duration is also longer. The concentration of drugs in brain tissue decreased gradually in the order of olfactory bulb, olfactory tract, brain and cerebellum.

After intravenous administration and intranasal administration of galantamine system, at the same time point, the drug concentration in brain tissue was far greater than that of the original drug of galantamine, and the duration was also longer. The concentration of drugs in brain tissue decreased gradually in the order of olfactory bulb, olfactory tract, brain, and cerebellum.

Table V. Concentration of galantamine original drug solution in olfactory bulb after intravenous injection and nasal administration.

Time (min)	Intravenous injection (ng/mL)	Nasal administration (ng/mL)
2	59.90±35.24	–
5	25.60±3.67	1,453.54±990.76
15	24.70±1.83	1,342.95±979.54
30	ND	731.02±159.56
60	ND	400.73±30.20
90	ND	191.70±38.71
120	ND	172.82±177.15
240	ND	51.90±6.13
360	ND	54.27±16.64
480	–	30.58±8.53

ND: not detected.

Table VI. Drug concentration of galantamine system solution in olfactory bulb after intravenous injection and nasal administration.

Time	Intravenous injection (ng/mL)	Nasal administration (ng/mL)
2 min	3,532.23±355.02	4,141.15±632.35
5 min	2,911.45±237.23	3,258.35±532.65
15 min	2,340.52±135.53	2,844.52±449.44
30 min	1,826.9±135.64	2,081.54±354.84
60 min	1,444.41±245.33	1,618.14±454.21
90 min	1,234.42±145.34	1,334.34±332.43
120 min	956.34±117.33	1,125.45±152.46
240 min	707.27±158.53	849.35±86.42
6 h	526.19±114.14	649.62±42.46
8 h	414.81±19.43	553.51±59.45
12 h	332.17±45.62	347.15±85.34
24 h	215.72±82.54	232.35±74.45
36 h	124.20±14.43	113.32±34.56

Table VII. Concentration of galantamine original drug solution in olfactory tract after intravenous injection and nasal administration.

Time (min)	Intravenous injection (ng/mL)	Nasal administration (ng/mL)
2	30.57±7.23	–
5	19.05±3.05	241.51±102.83
15	ND	111.21±48.44
30	ND	43.81±29.33
60	ND	22.23±6.89
90	ND	ND
120	ND	ND
240	ND	ND
360	ND	ND
480	–	ND

ND: not detected.

Table VIII. Concentration of galantamine system solution in olfactory tract after intravenous injection and nasal administration.

Time	Intravenous injection (ng/mL)	Nasal administration (ng/mL)
2 min	2,532.41±347.51	3,732.45±569.44
5 min	2,458.14±343.45	3,046.25±246.34
15 min	1,439.43±535.34	2,537.44±545.46
30 min	1,629.71±437.82	1,778.45±456.31
60 min	1,462.47±444.55	1,468.46±451.14
90 min	947.54±134.31	1,207.44±349.53
120 min	734.16±140.34	1,014.26±434.61
240 min	542.43±141.43	760.01±324.41
6 h	415.52±143.56	575.61±104.32
8 h	342.34±145.44	503.67±135.45
12 h	269.43±142.42	354.85±173.23
24 h	190.75±83.35	245.32±97.16
36 h	96.56±65.83	153.73±72.24

Table IX. Brain drug concentration of galantamine original drug solution after intravenous injection and nasal administration.

Time	Intravenous injection (ng/mL)	Nasal administration (ng/mL)
2	24.48±3.84	–
5	23.15±4.76	23.46±3.11
15	ND	18.58±3.58
30	ND	19.77±0.94
60	ND	22.75±1.18
90	ND	ND
120	ND	ND
240	ND	ND
360	ND	ND
480	–	ND

ND: not detected.

In the brain tissues of the olfactory bulb, olfactory tract, cerebrum, and cerebellum, the drug concentration of the galantamine system after intravenous injection is lower than that after nasal administration. Therefore, nasal administration can transmit more medicine.

Comprehensively comparing the results in Tables V to XII, it can be seen that the effect of the galantamine system in the delivery of the drug in the brain tissue is much higher than that of the galantamine original drug.

Brain Targeting Evaluation of Galantamine Nano System After Intranasal Administration

The galantamine original drug solution and galantamine system solution were administered intravenously and nasally to rats, respectively. The AUC values of the drugs in different parts are shown in Table XIII. The calculation results of DTI are shown in Table XIV, which reflects the evaluation index of brain targeting.

It was shown that the DTI of galantamine original drug after intranasal administration is also greater than 1 in the olfactory bulb, brain, and cerebellum and has certain brain targeting properties ($p<0.05$). This may be due to the fact that galantamine is a small-molecule drug and can reach the brain through the nasal cavity by itself.

Discussion

From the results of blood concentration of galantamine original drug solution and system solution after intravenous injection and nasal administration, it is known that in the serum, the galantamine system has a sustained release effect compared to the original drug. However, at the same time point, the plasma concentration of the

Table X. Brain drug concentration of galantamine system solution after intravenous injection and nasal administration.

Time	Intravenous injection (ng/mL)	Nasal administration (ng/mL)
2 min	2,452.40±223.35	3,208.93±328.52
5 min	1,474.34±111.78	2,884.23±261.45
15 min	1,626.67±133.73	2,422.72145.61
30 min	1,245.38±221.63	1,571.13±134.67
60 min	971.32±130.19	1,373.21±145.53
90 min	837.62±183.21	1,151.34±113.17
120 min	614.01±95.34	919.35±238.14
240 min	457.24±71.34	732.15±160.45
6 h	336.56±54.46	524.45±245.56
8 h	249.42±64.68	412.15±160.15
12 h	213.54±46.35	332.34±59.95
24 h	130.11±32.13	178.45±73.45
36 h	71.06±82.34	140.34±43.63

ND: not detected.

Table XI. Concentration of galantamine original drug solution in cerebellum after intravenous injection and nasal administration..

Time (min)	Intravenous injection (ng/mL)	Nasal administration (ng/mL)
2	33.23±7.41	–
5	31.00±3.80	24.23±5.58
15	ND	16.36±1.15
30	ND	24.72±1.61
60	ND	ND
90	ND	ND
120	ND	ND
240	ND	ND
360	ND	ND
480	–	ND

ND: not detected.

galantamine system was not higher than that of the original galantamine drug but lower, which indicated that the peripheral concentration of the drug decreased after the system was formed, and the peripheral toxicity would decrease.

After intranasal administration of the galantamine system, the DTI in the olfactory bulb, olfactory tract, brain, and cerebellum is much larger than that of the original drug. The galantamine system has obvious brain targeting, and the brain targeting index at the olfactory bulb is the largest, and the targeting is the best.

In addition, from the drug concentration of the galantamine system in rat brain tissue after intravenous injection in the previous section, it can be seen that there is also brain targeting after intravenous injection, which is higher than that of the original galantamine drug.

The galantamine system has better brain targeting than the original galantamine drug, which may be attributed to its strong adsorption[24,25] and permeability with the nasal mucosal layer.

Conclusions

Simultaneously analyzing the blood drug concentration and brain tissue drug concentration after intravenous injection of the original drug solution and system solution and nasal administration, and calculating DTI of the olfactory bulb, olfactory tract, brain, and cerebellum after nasal administration, it was found that compared with the original drug solution, the nano-drug-loading system has obvious brain-targeting properties for nasal administration, and intravenous administration also has brain-targeting properties. In the olfactory bulb, olfactory tract, brain, and cerebellum, the brain targeting index at the olfactory bulb is the largest, and the targeting is the best.

Table XII. Concentration of galantamine system solution in cerebellum after intravenous injection and nasal administration.

Time	Intravenous injection (ng/mL)	Nasal administration (ng/mL)
2 min	1,344.35±352.33	1,766.45±331.42
5 min	1,223.72±422.17	1,419.54±216.24
15 min	1,128.23±239.32	1,240.36±224.47
30 min	717.26±146.42	922.58±241.34
60 min	657.45±135.12	710.13±137.12
90 min	573.34±94.34	544.35±155.83
120 min	412.31±89.28	522.31±134.55
240 min	335.46±33.32	335.48±144.23
6 h	218.23±35.29	238.42±61.12
8 h	135.32±24.35	234.12±40.34
12 h	146.21±24.24	120.41±25.28
24 h	85.24±24.53	117.32±47.22
36 h	43.41±7.43	53.24±4.46

Table XIII. AUC values of galantamine original drug solution and its system solution at different parts after intravenous injection and nasal administration.

Route of administration	Drug type	Parts of rats	AUC_{0-t} (ng.min.ml^{-1})	$AUC_{brain\ tissue}/AUC_{plasma}$ (%)
Intravenous injection	Galantamine original drug	Plasma	140,325.35	100
		Olfactory bulb	400.65	0.29
		Olfactory tract	125.02	0.09
		Brain	98.95	0.07
		Cerebellum	139.59	0.10
	Galantamine system	Plasma	63,590.32	100
		Olfactory bulb	243,512.60	382.94
		Olfactory tract	5,352.35	8.42
		Brain	1,244.43	1.96
		Cerebellum	687.35	1.08
Nasal administration	Galantamine original drug	Plasma	150,148.12	100
		Olfactory bulb	480.78	0.32
		Olfactory tract	136.27	0.09
		Brain	128.63	0.09
		Cerebellum	181.46	0.12
	Galantamine system	Plasma	64,371.62	100
		Olfactory bulb	9,324,460.35	14,485.36
		Olfactory tract	82,260.46	127.79
		Brain	36,421.43	56.58
		Cerebellum	18,649.46	28.97

Table XIV. Brain targeting index of galantamine original drug and its system solution after intravenous injection and nasal administration.

Brain tissue	Galantamine original drug	Galantamine system
Olfactory bulb	1.1	37.8*
Olfactory tract	1.0	15.2*
Brain	1.2	28.9*
Cerebellum	1.2	26.8*

*$p<0.05$.

Conflict of Interest
The authors declare that they have no conflict of interest.

Acknowledgments
The authors wish to thank all the colleagues who participated in the study.

Informed Consent
Not applicable.

Ethics Approval
The Animal Welfare and Ethics of Chongqing Western Biomedical Technology Co., Ltd, China (WST. No. 20200210S032033[001]) approved the research protocol, and the research was conducted according to the criteria mentioned in the ARRIVE guidelines.

Funding
This work was supported by financial support from the major new drug innovation project of the Ministry of Science and Technology of China (No. 2017ZX09301001), the China Central Finance Improvement Project for the National Key Laboratory of Traditional Chinese Medicine [China Central Finance CS (2021) No. 151], the Special Key Project of Science and Technology of Guangdong Province with Strong Traditional Chinese medicine (No. 20215002), Shenzhen Science and Technology Program (No. JCYJ20230807115305011, No. JCYJ 20210324122200002, and No. JCYJ 20150401171152771).

Data Availability
The datasets used and/or analyzed during the current study are available from the corresponding author upon reasonable request.

Authors' Contributions
Lihong Duan: conceptualization, methodology, funding acquisition, writing-original draft preparation. Limin Li: experiment. Chunbao Wang: resources, software. Quanquan Liu: conceptualization, supervision. Xin Zhang: resources, formal analysis. Zhengzhi Wu: funding acquisition, writing- review and editing.

ORCID ID
Lihong Duan: 0000-0002-4840-6873
Limin Li: 0009-0009-4199-4658
Chunbao Wang: 0000-0002-8795-0142
Quanquan Liu: 0000-0002-2044-6160
Xin Zhang: 0000-0002-7246-2410
Zhengzhi Wu: 0000-0001-7547-4647

References

1) Shakir MN, Dugger BN. Advances in Deep Neuropathological Phenotyping of Alzheimer Disease: Past, Present, and Future. J Neuropathol Exp Neurol 2022; 81: 2-15.
2) Bortolami M, Rocco D, Messore A, Santo RD, Costi R, Madia VN, Scipione L, Pandolfi F. Acetylcholinesterase inhibitors for the treatment of Alzheimer's disease - a patent review (2016-present). Expert Opin Ther Pat 2021; 31: 399-420
3) Patterson C. World Alzheimer report 2018. In: the state of the art of dementia research: new frontiers. Alzheimer's Disease International. London, UK: Alzheimer's Disease International (ADI) 2018; 32-36.
4) Mendez MF, Cherrier MM, Meadows RS. Depth perception in Alzheimer's disease. Percept Mot Skills 1996; 83: 987-995.
5) Wang S, Yan D, Temkin-Greener H, Cai SB. Nursing home admissions for persons with dementia: Role of home- and community-based services. Health Serv Res 2021; 56: 1168-1178.
6) Liu C, Guo X, Chang X. Intestinal Flora Balance Therapy Based on Probiotic Support Improves Cognitive Function and Symptoms in Patients with Alzheimer's Disease: A Systematic Review and Meta-analysis. Biomed Res Int 2022; 2022: 4806163.
7) Frith E, Loprinzi PD. Physical activity is associated with higher cognitive function among adults at risk for Alzheimer's disease. Complement Ther Med 2018; 36: 46-49.
8) Song L, Li X, Bai XX. Calycosin improves cognitive function in a transgenic mouse model of Alzheimer's disease by activating the protein kinase C pathway. Neural Regen Res 2017; 12: 1870-1876.
9) Zhang Y, Noh K, Song W. Chinese herbal medicines on cognitive function and activity of daily living in senior adults with Alzheimer's disease: a systematic review and meta-analysis. Integr Med Res 2019; 8: 92-100.
10) Bierman EJ, Comijs HC, Jonker C. The effect of anxiety and depression on decline of memory function in Alzheimer's disease. Int Psychogeriatr 2009; 21: 1142-1147.
11) Souchay C, Moulin CJ. Memory and consciousness in Alzheimer's disease. Curr Alzheimer Res 2009; 6: 186-195.
12) Ferris SH, Farlow M. Language impairment in Alzheimer's disease and benefits of acetylcholinesterase inhibitors. Clin Interv Aging 2013; 8: 1007-1014.
13) Vasenina EE, Veryugina NI, Levin OS. Capabilities of combined therapy of Alzheimer's disease. Zh Nevrol Psikhiatr Im S S Korsakova 2022; 122: 45-50.
14) Zeyadi M, Al-abbasi FA, Afzal M, Bawadood AS, Sheikh RA, Alzarea SI, Sayyed N, Kazmi I. Butin attenuates behavioral disorders via cholinergic/BDNF/Caspase-3 pathway in scopolamine-evoked memory deficits in rats. Eur Rev Med Pharmacol Sci 2024; 28: 981-994.

15) WU ZZ, Huang ACJ, Vellis JD. Effect of Tiantai No.1 on Neurotoxicity of β-Amyloid and NFκB and cAMP/CREB Pathways. Chin J Integr Med 2008; 14: 286-292.

16) Wu ZZ, Li M, Huang ACJ, Jia XQ, Li YH, Chen MY. Effects of serum containing natural Cerebrolysin on glucose-regulated protein 78 and CCAAT enhancer-binding protein homologous protein expression in neuronal PC12 cells following tunicamycin-induced endoplasmic reticulum stress. Neural Regen Res 2009; 4: 92-97.

17) Wu ZZ, LI YH, Cao MQ, Li M, Sun KH, Yang M, Chuan MY, Huang ACJ. Effect of Natural Brain-Kenetine on Variance of Gene Expression Profiles in Hippocampus of AD Rats Analyzed by Genome Chips and Bioinformatics Techniques. Proceeding of 2008 International Symposium on IT in Medicine and Education 2008; 730-737. Available at: https://ieeexplore.ieee.org/document/4743963

18) Li YH, Wu ZZ, Gao XW, Zhu QW, Jin Y, Wu AM, Huang ACJ. Anchanling reduces pathology in a lactacystin-induced Parkinson's disease model. Neural Regen Res 2012; 7: 165-170.

19) Jeong SH, Jang JH, Lee YB. Drug delivery to the brain via the nasal route of administration: exploration of key targets and major consideration factors. J Pharm Investig 2022; 53: 1-34.

20) Scherließ R. Nasal formulations for drug administration and characterization of nasal preparations in drug delivery. Ther Deliv 2020; 11: 183-191.

21) Davis SS, Illum L. Absorption enhancers for nasal drug delivery. Clin Pharmacokinet 2003; 42: 1107-1128.

22) Illum L. Nasal drug delivery-Possibilities, problems and solutions. J Control Release 2003; 87: 187-198.

23) Illum L. Nasal drug delivery: new developments and strategies. Drug Discov Today 2002; 7: 1184-1189.

24) Aspden TJ, Adier J, Davis SS, Skaugrud, Illum L. Chitosan as a nasal delivery system: evaluation of the effect of chitosan on mucociliary clearance rate in the frog palate model. Int J Phann 1995; 122: 69-78.

25) Takeuchi H, Yamamoto H, Kawashima Y. Mucoadhesive nanoparticulate systems for peptide drug delivery. Adv Deliv Rev 2001; 47: 39-54.

26) Artursson P, Lindmark T, Davis SS, Illum L. Effect of chitosan on the permeability of monolayers of intestinal epithelial cells (Caco-2). Pharm Res 1994; 11: 1358-1361.

27) Zhang YB, Wang Y, Liu YN, Gong TX, Hou MX. The Anti-inflammatory Effect of Chitosan Oligosaccharide on Heart Failure in Mice. Biomed Res Int 2022; 2022: 8746530.

28) Narvaez-Flores JJ, Vilar-Pineda G, Acosta-Torres LS, Garcia-Contreras R. Cytotoxic and anti-inflammatory effects of chitosan and hemostatic gelatin in oral cell culture. Acta Odontol Latinoam 2021; 34: 98-103.

29) Yoon HJ, Moon ME, Park HS, Im SH, Kim YH. Chitosan oligosaccharide (COS) inhibits LPS-induced inflammatory effects in RAW 264.7 macrophage cells. Biochem Biophys Res Commun 2007; 358: 954-959.

30) Duan LH, Wang CB, Li YH, Wu ZZ, Li LM, Zhang XL. A study on the nasal mucosal toxicity and nasal mucosal absorption of a novel drug delivery system. Shenzhen J Inte Trad Chin West Med 2020; 30: 1-5.

31) SakaneT, Yamashita S, Yata N, Sezaki H. Transnasal delivery of 5-fluorouracil to the brain in the rat. J Drug Target 1997; 7: 233-240.

32) Wang F, Jiang X, Lu W. Profiles of methotrexate in blood and CSF following intranasal and intravenous administration to rats. Int J Pharm 2003; 263: 1-7.

33) Lee KY, Bouhadir KH, Mooney DJ. Evaluation of Chain Rigidity of Partially Oxidized Polyguluronate. Biomacromolecules 2002; 3: 1129.

34) Scott JE, Page-Thomas DP. Spectrofluorimetric detection and measurement of hydroxyl radicals in periodate solution. Carbohydr Res 1976; 52: 214-218.